NUMERICAL SOLUTION OF MULTIMEDIUM FLOW WITH VARIOUS DISCONTINUITIES*

WU XIONG-HUA (吴雄华), ZHU YOU-LAN (朱幼兰)
(*Computing Center, Academia Sinica, Beijing, China*)

1. Introduction

In this paper we discuss the numerical solution of the interaction of the strong plane explosion wave with the boundary between two gases.

Because this kind of unsteady problem has a characteristic length and there are shocks, contact discontinuities and rarefaction waves, it is a good test problem for judging methods.

The singularity-separating method presented in [1] can accurately solve this kind of problem. Its scheme is unconditionally stable and possesses a second order accuracy. We have obtained satisfactory numerical results using the singularity-separating method for this complicated problem.

We shall show the singularity-separating method and its difference scheme in detail. Also we shall give the fractional errors of mass, momentum and energy for our numerical results. The error estimations show that our solutions are accurate.

Finally, we shall compare this method with the *L-W* scheme for a special problem.

2. Formulation of the Problem

We consider the following problem of plane unsteady motion of a perfect gas. The system of equations of gas dynamics is

$$\begin{cases} \dfrac{\partial u}{\partial t}+u\dfrac{\partial u}{\partial x}+\dfrac{1}{\rho}\dfrac{\partial p}{\partial x}=0, \\ \dfrac{\partial \rho}{\partial t}+u\dfrac{\partial \rho}{\partial x}+\rho\dfrac{\partial u}{\partial x}=0, \\ \dfrac{\partial p}{\partial t}+u\dfrac{\partial p}{\partial x}+\gamma p\dfrac{\partial u}{\partial x}=0. \end{cases} \tag{1}$$

Suppose that at the time $t=-t_1(t_1>0)$, the state of flow field is $\gamma=\gamma_l$ (ratio of specific heats), $\rho=\rho_l$ (density), $u=u_l=0$ (velocity), $p=p_l=0$ (pressure), $e=e_l=0$ (internal energy) at $x<0$ and $\gamma=\gamma_r$, $\rho=\rho_r$, $u=u_r=0$, $p=p_r=0$, $e=e_r=0$ at $x>0$. There is a strong explosion on the plane $x=R_0$ (see Fig. 1). "Strong" explosion means that the internal energy and the pressure of the static gas in front of the explosion wave can be neglected as compared with the energy released per unit area E. The explosion wave AO moves towards the boundary of two gases. It meets the boundary

* Received September 21, 1982.

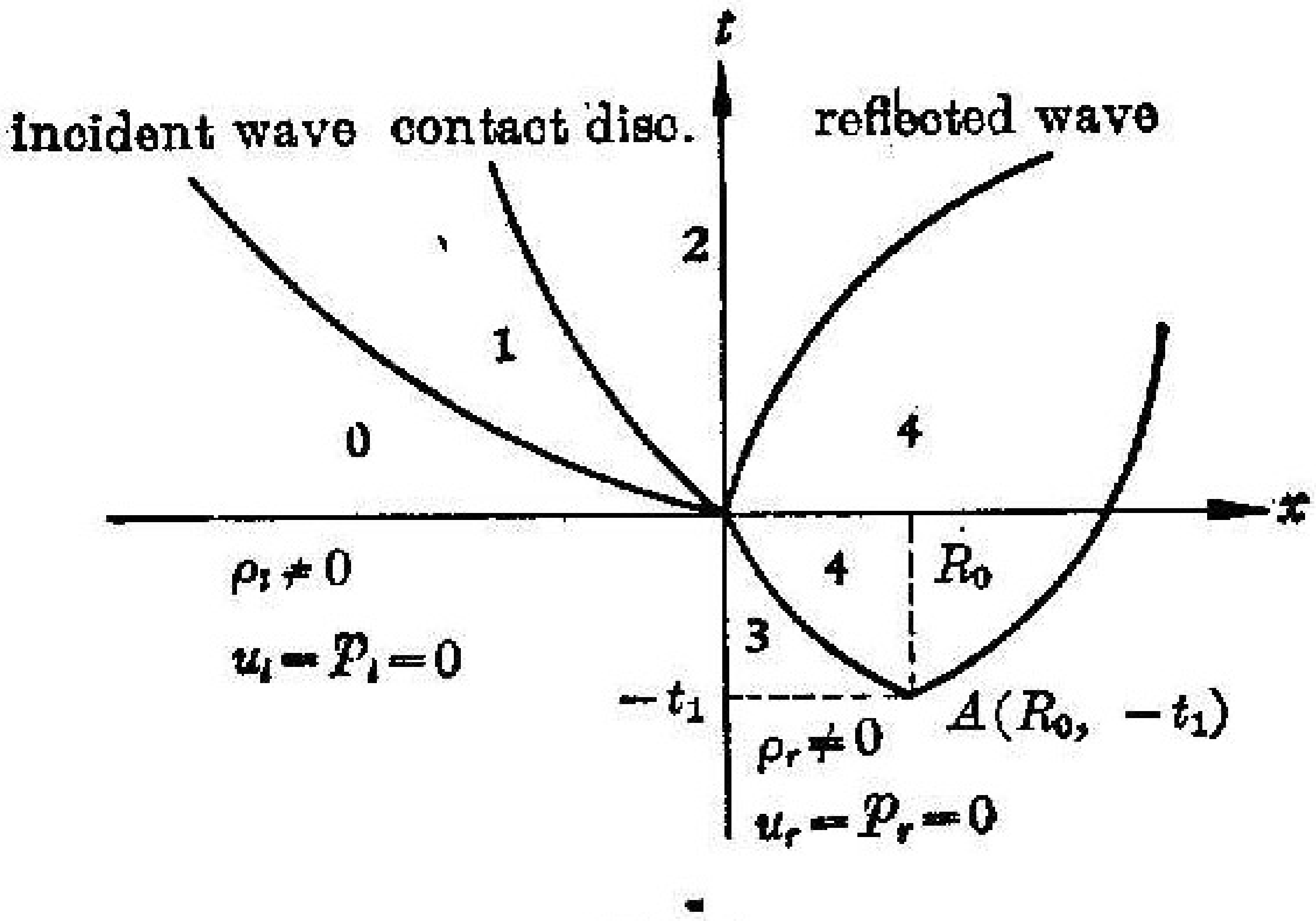

Fig. 1

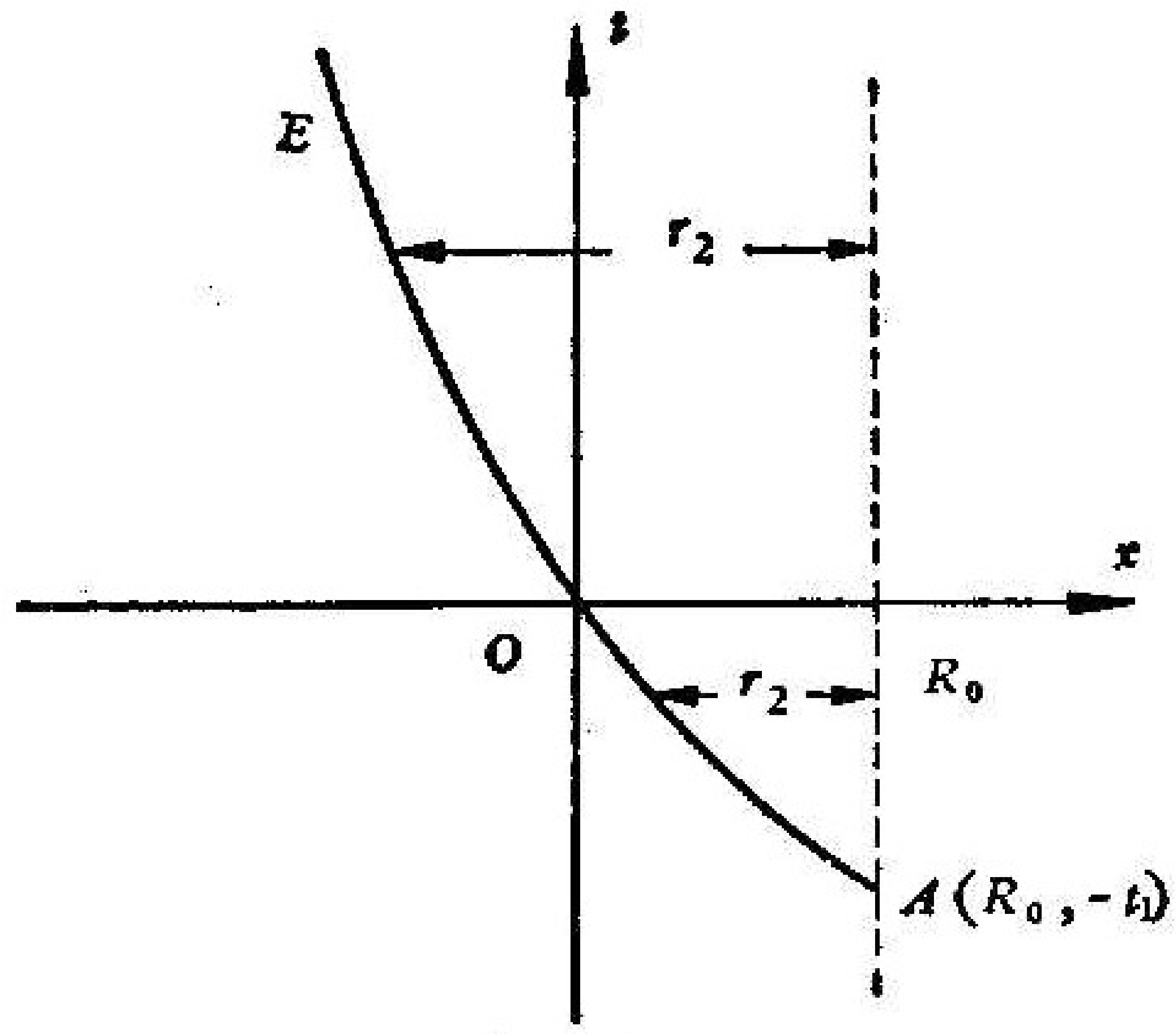

Fig. 2

at $t=0$. As a result of interaction, an incident shock, a contact discontinuity and a reflected wave (rarefaction wave or shock wave) are produced.

There is a self-similar solution in region 4 because the internal energy and the pressure of the static gas in front of the explosion wave are zero. Its analytic expressions are given in [2] and [3]. The curve AOE in Fig. 2 represents the incident shock. Let r_2 denote the distance between OE and $x=R_0$. According to those expressions, we have

$$r_2=\left(\frac{E}{\rho_r}\right)^{1/3}(t+t_1)^{2/3},$$

$$\frac{dr_2}{dt}=V=\frac{2}{3}\frac{r_2}{t+t_1}$$

(V is the velocity of explosion wave) and

$$R_0=\left(\frac{E}{\rho_r}\right)^{1/3}t_1^{2/3}.$$

Put $R_0=0.1\,\mathrm{m}$, $E=2734905.6\,\mathrm{J/m^2}$, $t_1=2.1718193\times10^{-5}\,\mathrm{s}$, $\rho_0=1.29\,\mathrm{kg/m^3}$ and the ratio of specific heats $\gamma=1.4$.

The shock relations are

$$\begin{cases}\rho_1(u_1-V)=\rho_0(u_0-V), & (2a)\\ \rho_1(u_1-V)^2+p_1=\rho_0(u_0-V)^2+p_0, & (2b)\\ e_1+\dfrac{1}{2}(u_1-V)^2+\dfrac{p_1}{\rho_1}=e_0+\dfrac{1}{2}(u_0-V)^2+\dfrac{p_0}{\rho_0}. & (2c)\end{cases}$$

Here the quantities with the subscript 0 denote the quantities in front of the wave, the quantities with the subscript 1 denote the quantities behind the wave, the internal energy $e_1=\frac{1}{\gamma-1}\frac{p_1}{\rho_1}$ and $u_0=e_0=p_0=0$. From (2) we obtain

$$\begin{cases}\rho_1(u_1-V)=-\rho_0V, & (3a)\\ \rho_1(u_1-V)^2+p_1=\rho_0V^2, & (3b)\\ \dfrac{\gamma}{\gamma-1}\dfrac{p_1}{\rho_1}+\dfrac{1}{2}(u_1-V)^2=\dfrac{1}{2}V^2. & (3c)\end{cases}$$

Furthermore, it follows from (3a—c) that

$$p_1=\rho_1u_1(V-u_1), \tag{4}$$

$$u_1=\frac{2}{\gamma+1}V, \tag{5}$$

$$\rho_1=\frac{\gamma+1}{\gamma-1}\rho \tag{6}$$

and

$$p_1=\frac{2}{\gamma+1}\rho_0 V^2. \tag{7}$$

If $\gamma=1.4$, it can be easily derived that behind the incident wave AOE the gas density $\bar{\rho}=6\rho_0$, the velocity of the gas $\bar{\nu}=\frac{V}{1.2}$ and the pressure $\bar{p}=\rho_0 V^2/1.2$. Denote $(R_0-x)/r_2$ by $R(x,t)$. It relates to a parameter $\tilde{V}$ by the relation[2]

$$R=(1.8\tilde{V})^{-2/3}(12.6\tilde{V}-6)^{2/9}(3-3.6\tilde{V})^{-5/9};$$

then u, ρ, p in region 4 can be expressed by

$$\begin{cases} u=-\bar{\nu}(1.8R\tilde{V}), & (8a)\\ \rho=\bar{\rho}(12.6\tilde{V}-6)^{5/9}(6-9\tilde{V})^{-10/3}(3-3.6\tilde{V})^{25/9}, & (8b)\\ p=\bar{p}(1.8\tilde{V})^{2/3}(6-9\tilde{V})^{-7/3}(3-3.6\tilde{V})^{5/3}. & (8c)\end{cases}$$

Our aim is to determine the quantities in the whole region from the incident wave to the reflected wave.

3. Numerical Methods

First we rewrite the system of equations (1) in the characteristic form

$$\begin{pmatrix} \rho c, & 0, & 1\\ 0, & \gamma p, & -\rho\\ -\rho c, & 0, & 1\end{pmatrix}\frac{\partial}{\partial t}\begin{pmatrix} u\\ \rho\\ p\end{pmatrix} + \begin{pmatrix} u+c, & 0, & 0\\ 0, & u, & 0\\ 0, & 0, & u-c\end{pmatrix}\begin{pmatrix} \rho c, & 0, & 1\\ 0, & \gamma p, & -\rho\\ -\rho c, & 0, & 1\end{pmatrix}\frac{\partial}{\partial x}\begin{pmatrix} u\\ \rho\\ p\end{pmatrix}=0,$$

i. e.

$$\tilde{G}\frac{\partial\tilde{U}}{\partial t}+\tilde{\Lambda}\tilde{G}\frac{\partial\tilde{U}}{\partial x}=0, \tag{9}$$

where

$$\tilde{G}=\begin{pmatrix} \rho c, & 0, & 1\\ 0, & \gamma p, & -\rho\\ -\rho c, & 0, & 1\end{pmatrix},\ \tilde{U}=\begin{pmatrix} u\\ \rho\\ p\end{pmatrix},\ \tilde{\Lambda}=\begin{pmatrix} \tilde{\lambda}_1, & 0, & 0\\ 0, & \tilde{\lambda}_2, & 0\\ 0, & 0, & \tilde{\lambda}_3\end{pmatrix}=\begin{pmatrix} u+c, & 0, & 0\\ 0, & u, & 0\\ 0, & 0, & u-c\end{pmatrix},$$

and sound velocity $c=\sqrt{\gamma p/\rho}$.

Suppose that there are $S+1$ discontinuity lines $x_i(t)\,(i=0,\cdots,S)$ in the region where we try to find the solution. A domain between $x_i(t)$ and $x_{i+1}(t)$ is called a subregion. Thus the computational region consists of S subregions. Obviously an arbitrary subregion whose boundaries are $x_i(t)$ and $x_{i+1}(t)$ can be transformed into a strip $i\leqslant\xi\leqslant i+1$ on the ξ–t plane by using the transformation $t=t$, $\xi=(x-x_i)/(x_{i+1}(t)-x_i(t))+i$. Because there are the following relations for $\tilde{U}(x,t)=U(\xi,t)$:

$$\frac{\partial U}{\partial t}=\frac{\partial t}{\partial t}\frac{\partial U}{\partial t}+\frac{\partial \xi}{\partial t}\frac{\partial U}{\partial \xi}=\frac{\partial U}{\partial t}+\frac{\partial \xi}{\partial t}\frac{\partial U}{\partial \xi},$$

$$\frac{\partial U}{\partial x}=\frac{\partial t}{\partial x}\frac{\partial U}{\partial t}+\frac{\partial \xi}{\partial x}\frac{\partial U}{\partial \xi}=\frac{\partial \xi}{\partial x}\frac{\partial U}{\partial \xi},$$

the system of equations in the new coordinates is

$$G\frac{\partial U}{\partial t}+\Lambda G\frac{\partial U}{\partial \xi}=0, \tag{10}$$

or

$$G_n\frac{\partial U}{\partial t}+\lambda_n G_n\frac{\partial U}{\partial \xi}=0, \quad n=1,\ 2,\ 3, \tag{11}$$

where,

$$G(\xi,\ t)=\tilde{G}(x,\ t), \qquad \Lambda=\begin{pmatrix}\lambda_1, & 0, & 0\\ 0, & \lambda_2, & 0\\ 0, & 0, & \lambda_3\end{pmatrix},$$

$$\lambda_n=\frac{\partial \xi}{\partial x}\tilde{\lambda}_n+\frac{\partial \xi}{\partial t}=\frac{1}{x_{i+1}(t)-x_i(t)}(\tilde{\lambda}_n-(\xi-i)(V_{i+1}(t)-V_i(t))),$$

$V_i(t)=\dfrac{dx_i(t)}{dt}$ is the speed of the i-th discontinuity front, and G_n is the n-th row of G. For simplicity we omit the subscript n of λ_n, G_n in the difference equations.

In what follows we use the following notation:

$\sigma=\lambda\Delta t/\Delta\xi$, $u^k_{s,m}=u(\xi_{s,m},\ t_k)$, $\xi_{s,m}=s+m\Delta\xi$, $m=0,\ 1,\ \cdots,\ M$, $M+1$ being the number of the mesh points in each subregion and the subscript s and the superscript k are sometimes omitted. Other quantities have similar denotations. There is an explicit-implicit-mixed scheme in [1]. It is suitable for various increments of the variables x and t. Here we compute problems using this scheme.

If $|\sigma|\leqslant 1$ we take the following explicit scheme: At the interim level the approximation formula is

$$G^k_m U^{k+\frac{1}{2}}_m=(1\mp\sigma^k_m/2)G^k_m U^k_m\pm(\sigma^k_m/2)G^k_m U^k_{m\mp1},$$

where we take the upper sign if $\sigma>0$ or the lower sign if $\sigma<0$; and at the regular level the formula is

$$\frac{1}{2}((1-B_m)(G^{k+\frac{1}{2}}_{m+1}+G^{k+\frac{1}{2}}_m)+B_m(G^{k+\frac{1}{2}}_m+G^{k+\frac{1}{2}}_{m-1}))U^{k+1}_m=(1-B_m)S^1_m+B_m S^2_m.$$

Here,

$$S^1_m=(G^{k+\frac{1}{2}}_m+G^{k+\frac{1}{2}}_{m+1})U^k_{m+1}/2-((\sigma^{k+\frac{1}{2}}_m+\sigma^{k+\frac{1}{2}}_{m+1})/2+1)$$
$$\cdot(G^{k+\frac{1}{2}}_m+G^{k+\frac{1}{2}}_{m+1})(U^{k+\frac{1}{2}}_{m+1}-U^{k+\frac{1}{2}}_m)/2,$$

$$S^2_m=(G^{k+\frac{1}{2}}_m+G^{k+\frac{1}{2}}_{m-1})U^k_{m-1}/2-((\sigma^{k+\frac{1}{2}}_m+\sigma^{k+\frac{1}{2}}_{m-1})/2-1)$$
$$\cdot(G^{k+\frac{1}{2}}_m+G^{k+\frac{1}{2}}_{m-1})(U^{k+\frac{1}{2}}_m-U^{k+\frac{1}{2}}_{m-1})/2,$$

$$B_m=\begin{cases} m/M_1, & 0\leqslant m<M_1,\\ \left.\begin{matrix}0 & \lambda>0\\ 1 & \lambda<0\end{matrix}\right\}, & M_1\leqslant m\leqslant M_2,\\ (m-M_1)/(M-M_2), & M_2<m\leqslant M,\end{cases}$$

$$M_1=\begin{cases} 0, & \lambda>0 \text{ on } \xi=0,\\ \min\left\{E\left(\frac{\xi_1}{\Delta\xi}\right),\ M-1\right\}, & \lambda\leqslant 0 \text{ on } \xi=0,\end{cases}$$

where ξ_1 is the maximum value among the values which make $\lambda \leqslant 0$ hold in the region $0 \leqslant \xi \leqslant \xi_1$ and $E(x)$ is the integral part of x, and

$$M_2 = \begin{cases} \max\left\{M - E\left(\frac{1-\xi_2}{\Delta\xi}\right),\ 1\right\}, & \lambda \geqslant 0 \text{ on } \xi = 1, \\ M, & \lambda < 0 \text{ on } \xi = 1, \end{cases}$$

where ξ_2 is the minimum value among the values which make $\lambda \geqslant 0$ hold in the region $\xi_2 \leqslant \xi \leqslant 1$.

If $|\sigma| > 1$, we take the following implicit scheme: At the interim level the formula is

$$(1 + (\sigma^k_{m+1} + \sigma^k_m)/2)(G^k_{m+1} + G^k_m)U^{k+\frac{1}{2}}_{m+1} + (1 - (\sigma^k_{m+1} + \sigma^k_m)/2)(G^k_{m+1} + G^k_m)U^{k+\frac{1}{2}}_m$$
$$= (G^k_{m+1} + G^k_m)(U^k_{m+1} + U^k_m);$$

and at the regular level the formula is

$$(1 + (\sigma^{k+\frac{1}{2}}_{m+1} + \sigma^{k+\frac{1}{2}}_m)/2)(G^{k+\frac{1}{2}}_{m+1} + G^{k+\frac{1}{2}}_m)U^{k+1}_{m+1}$$
$$+ (1 - (\sigma^{k+\frac{1}{2}}_{m+1} + \sigma^{k+\frac{1}{2}}_m)/2)(G^{k+\frac{1}{2}}_{m+1} + G^{k+\frac{1}{2}}_m)U^{k+1}_m$$
$$= (G^{k+\frac{1}{2}}_{m+1} + G^{k+\frac{1}{2}}_m)(U^k_{m+1} + U^k_m)$$
$$- (\sigma^{k+\frac{1}{2}}_{m+1} + \sigma^{k+\frac{1}{2}}_m)(G^{k+\frac{1}{2}}_{m+1} + G^{k+\frac{1}{2}}_m)(U^k_{m+1} - U^k_m).$$

This scheme has second order accuracy. Its stability has been discussed in [1].

Case I. Suppose that an incident shock wave ($x_1(t)$), a contact discontinuity($x_2(t)$) and a reflected rarefaction wave (between $x_3(t)$ and $x_4(t)$) are produced (see Fig. 3) when the strong explosion wave meets the boundary. Since the quantities in region 0 are known and the ones in region 4 can be obtained using (8a—c), what we must compute is the quantities in regions 1, 2, 3 and the locations and velocities of four discontinuity boundaries. In the following if u is a constant at a certain time in the s-th subregion we denote $\hat{u}_s$ as the speed of gas in this subregion and for ρ, p the same notation is used. Clearly we can compute the initial values in the regions in the following way. As well-known, from (5), (6), (7) and since the quantities are constant in region 1 at $t=0$, we know that

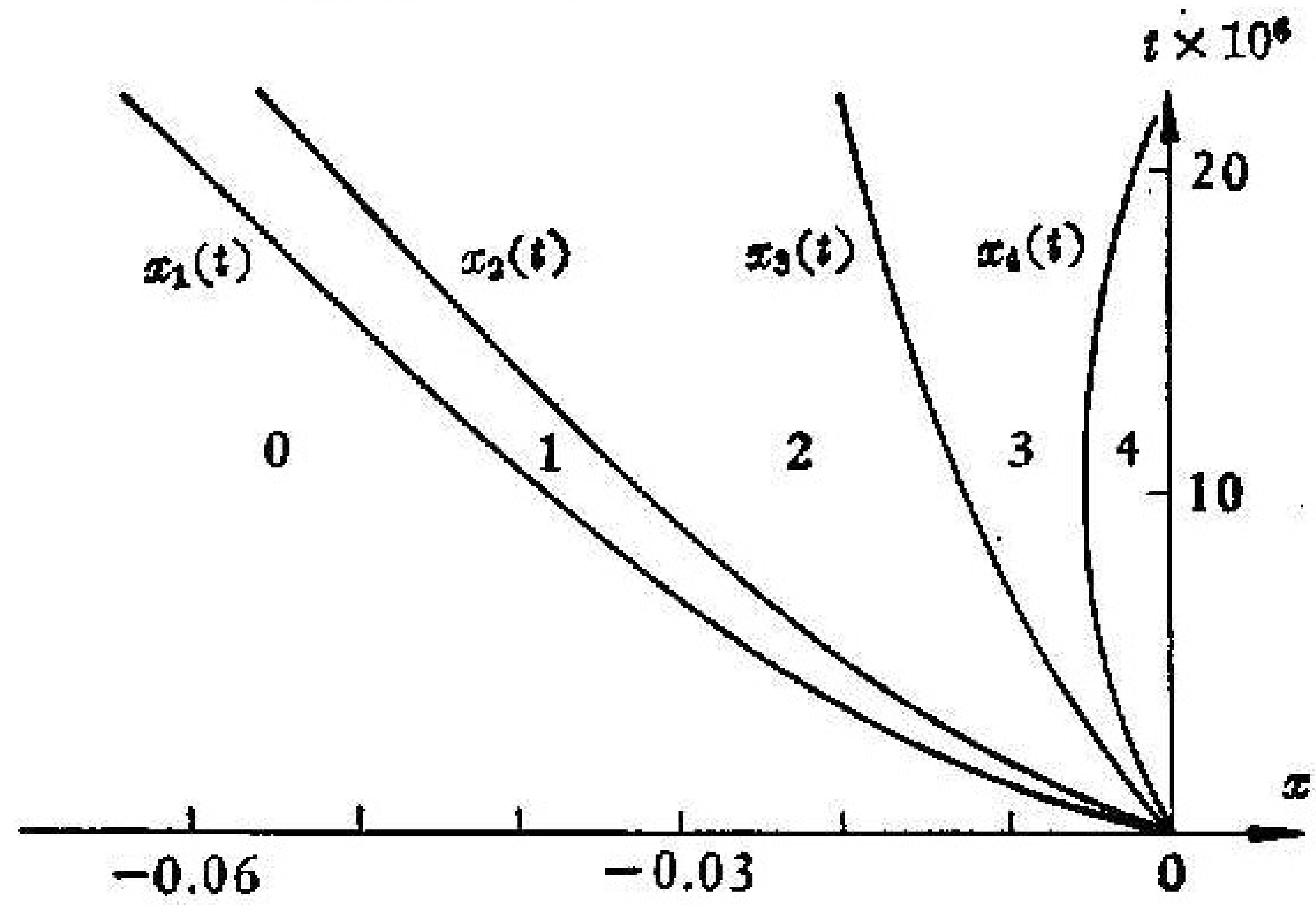

Fig. 3

$$\hat{\rho}_1 = \frac{\gamma+1}{\gamma-1}\rho_0, \quad \hat{u}_1 = \frac{2}{\gamma+1}V_1, \quad \hat{p}_1 = \frac{2}{\gamma+1}\rho_0 V_1^2 = \frac{\gamma+1}{2}\rho_0 \hat{u}_1^2.$$

From the contact discontinuity relations and the fact that the quantities are constant in region 2 at $t=0$ we have

$$\hat{u}_1 = \hat{u}_2, \quad \hat{p}_1 = \hat{p}_2;$$

and according to the relations of rarefaction wave, there are the relations:

$$c_{3,m} = c_{3,M} + \frac{\gamma_r - 1}{2}(u_{3,m} - u_{3,M}), \tag{12}$$

$$p_{3,m}=p_{3,M}\left(1+\frac{\gamma_r-1}{2}\frac{u_{3,m}-u_{3,M}}{c_{3,M}}\right)^{2\gamma_r/(\gamma_r-1)}, \tag{13}$$

$$\rho_{3,m}=\rho_{3,M}\left(1+\frac{\gamma_r-1}{2}\frac{u_{3,m}-u_{3,M}}{c_{3,M}}\right)^{2/(\gamma_r-1)}. \tag{14}$$

In addition, since the quantities at the boundary lines of the rarefaction wave are continuous, there are the relations:

$$\hat{u}_2=u_{3,0},\qquad \hat{\rho}_2=\rho_{3,0},\qquad \hat{p}_2=p_{3,0},$$

$$u_{3,M}=u_{4,0},\qquad \rho_{3,M}=\rho_{4,0},\qquad p_{3,M}=p_{4,0}.$$

From these relations we can derive

$$\hat{u}_1=\hat{u}_2=u_{3,0},\quad \hat{p}_1=\hat{p}_2=p_{3,0},$$

and

$$\hat{p}_1=\frac{\gamma+1}{2}\rho_0\hat{u}_1^2=p_{4,0}\left(1+\frac{\gamma_r-1}{2}\frac{\hat{u}_1-u_{4,0}}{c_{4,0}}\right)^{2\gamma_r/(\gamma_r-1)},$$

from which $\hat{u}_1$ and $\hat{p}_1$ can be determined. Using (14) with $m=0$ we can further obtain $\rho_{3,0}$, and $\rho_2=\rho_{3,0}$. Therefore the initial values in regions 1 and 2 can be easily determined. The initial values in region 3 can be computed by the following formulae. Since $c=\sqrt{\gamma p/\rho}$, the sound speeds $c_{3,0}$ and $c_{3,M}$ can be known. One of the relations of coordinate transformation in region 3 can be rewritten as

$$x=(\xi-3)x_4(t)+(4-\xi)x_3(t).$$

Differentiating this relation with respect to t yields

$$\frac{dx}{dt}=(\xi-3)\frac{dx_4(t)}{dt}+(4-\xi)\frac{dx_3(t)}{dt}.$$

Since $\frac{dx}{dt}$ should be always equal to $u+c$, taking $\xi=\frac{m}{M}+3$, $m=0, 1, \cdots, M$, we obtain

$$u_{3,m}+c_{3,m}=\frac{m}{M}(u_{3,M}+c_{3,M})+\left(1-\frac{m}{M}\right)(u_{3,0}+c_{3,0}). \tag{15}$$

Now we can easily obtain the formulae required. In fact from (12) and (15) we can derive

$$u_{3,m}=\left(\frac{m}{M}(u_{3,M}+c_{3,M})+\left(1-\frac{m}{M}\right)(u_{3,0}+c_{3,0})-c_{3,0}+\frac{\gamma_r-1}{2}u_{3,M}\right)\frac{2}{\gamma_r+1}, \tag{16}$$

and $p_{3,m}$ and $\rho_{3,m}$ can be determined immediately from (13) and (14). As for the velocities of four boundaries, clearly, they should be

$$V_1=\frac{\gamma_l+1}{2}u_{1,0},\quad V_2=u_{2,0},\quad V_3=u_{3,0}+c_{3,0},\quad V_4=u_{3,M}+c_{3,M}.$$

If $\lambda|_{\xi=s}>0$, $\lambda|_{\xi=s+1}\geqslant 0$ in the region $s\leqslant\xi\leqslant s+1$, we call the corresponding equation (11) the model problem A_1. If $\lambda|_{\xi=s}\leqslant 0$, $\lambda|_{\xi=s+1}<0$, we call it the model problem A_2. If $\lambda|_{\xi=s}\leqslant 0$, $\lambda|_{\xi=s+1}\geqslant 0$, we call it the model problem B (If $\lambda|_{\xi=s}>0$, $\lambda|_{\xi=s+1}<0$, we can split this region into two subregions, any one of which will belong to A_1 or A_2, by adding a corresponding characteristic line to this region). As pointed out above, we use the explicit-implicit scheme in [1] in our calculation. Since $|\lambda|$ corresponding to a model B is usually not large and $|\sigma|$ is usually less than 1, the explicit scheme is used at almost every point for the model B. In the following, we assume that Δt will be properly chosen so that the explicit scheme will be used at every point for the model problem B.

The three equations of (11) in region 1 belong respectively to the problems A_1, A_1, A_2. The ones in region 2 belong to the problems A_1, B, A_2. The ones in region 3 belong to the problems B, A_2, A_2. The systems of difference equations can be therefore written as follows:

$$\begin{cases} G_{11}^{(m+1)}U_{1,m+1}+\Omega_{11}^{(m+1)}G_{11}^{(m+1)}U_{1,m}=F_{11}^{(m+1)}, \\ G_{12}^{(m+1)}U_{1,m+1}+\Omega_{12}^{(m+1)}G_{12}^{(m+1)}U_{1,m}=F_{12}^{(m+1)}, \\ \Omega_{13}^{(m)}G_{13}^{(m)}U_{1,m+1}+G_{13}^{(m)}U_{1,m}=F_{13}^{(m)}, \\ \qquad m=0,\ 1,\ \cdots,\ M-1; \end{cases} \tag{17}$$

$$\begin{cases} G_{21}^{(m+1)}U_{2,m+1}+\Omega_{21}^{(m+1)}G_{21}^{(m+1)}U_{2,m}=F_{21}^{(m+1)}, & m=0,\ 1,\ \cdots,\ M-1, & (18a) \\ G_{22}^{(m)}U_{2,m}=F_{22}^{(m)}, & m=0,\ 1,\ \cdots,\ M, & (18b) \\ \Omega_{23}^{(m)}G_{23}^{(m)}U_{2,m+1}+G_{23}^{(m)}U_{2,m}=F_{23}^{(m)}, & m=0,\ 1,\ \cdots,\ M-1; & (18c) \end{cases}$$

$$\begin{cases} G_{31}^{(m)}U_{3,m}=F_{31}^{(m)}, & m=0,\ 1,\ \cdots,\ M, & (19a) \\ \Omega_{32}^{(m)}G_{32}^{(m)}U_{3,m+1}+G_{32}^{(m)}U_{3,m}=F_{32}^{(m)}, & m=0,\ 1,\ \cdots,\ M-1, & (19b) \\ \Omega_{33}^{(m)}G_{33}^{(m)}U_{3,m+1}+G_{33}^{(m)}U_{3,m}=F_{33}^{(m)}. & m=0,\ 1,\ \cdots,\ M-1; & (19c) \end{cases}$$

Here, $\Omega_{sn}^{(m)}=0$ when the explicit scheme is used, $\Omega_{sn}^{(m)}=(1-|\sigma_m+\sigma_{m+1}|/2)/(1+|\sigma_m+\sigma_{m+1}|/2)$ when the implicit scheme is used, σ is the one corresponding to the n-th characteristic value in the s-th region. Since $u_{3,M}$, $\rho_{3,M}$, $p_{3,M}$ can easily be determined by (8a—c), the system of equations (19) can be solved directly. Therefore we need to use the double-sweep method only for (17) and (18). We take (18) as an example to show the concrete process of the double-sweep method, which can be divided into the following three steps.

1) The process of elimination.

Let
$$\mu_0^{(1)}=G_{21}^{(1)},\qquad \mu_1^{(1)}=\Omega_{21}^{(1)}G_{21}^{(1)},\quad \mu^{(1)}=F_{21}^{(1)},$$
$$\nu_0^{(1)}=\Omega_{23}^{(0)}G_{23}^{(0)},\quad \nu_1^{(1)}=G_{23}^{(0)},\qquad \nu^{(1)}=F_{23}^{(0)};$$

then equations (18a) and (18c) with $m=0$ can be rewritten as follows:

$$\begin{cases} \mu_0^{(1)}U_{2,1}+\mu_1^{(1)}U_{2,0}=\mu^{(1)}, \\ \nu_0^{(1)}U_{2,1}+\nu_1^{(1)}U_{2,0}=\nu^{(1)}. \end{cases}$$

These two equations and (18a—c) with $m=1$ can be written in the following form with $m=1$:

$$\begin{cases} G_{21}^{(m+1)}U_{2,m+1}+\Omega_{21}^{(m+1)}G_{21}^{(m+1)}U_{2,m}=F_{21}^{(m+1)}, & (20a) \\ G_{22}^{(m)}U_{2,m}=F_{22}^{(m)}, & (20b) \\ \Omega_{23}^{(m)}G_{23}^{(m)}U_{2,m+1}+G_{23}^{(m)}U_{2,m}=F_{23}^{(m)}, & (20c) \\ \mu_0^{(m)}U_{2,m}+\mu_1^{(m)}U_{2,0}=\mu^{(m)}, & (20d) \\ \nu_0^{(m)}U_{2,m}+\nu_1^{(m)}U_{2,0}=\nu^{(m)}. & (20e) \end{cases}$$

The so-called elimination process is that for (20a—e) the following calculation is carried out. By using the pivoting-elimination method, from (20b—d) we obtain

$$U_{2,m}=G^{(m)^{-1}}\tilde{\tilde{F}}^{(m)}-\tilde{\tilde{G}}^{(m)^{-1}}\tilde{\tilde{H}}^{(m)}U_{2,m+1}-\tilde{\tilde{G}}^{(m)^{-1}}\tilde{\tilde{\mu}}^{(m)}U_{2,0}, \tag{21}$$

where

$$\tilde{\tilde{G}}^{(m)}=\begin{pmatrix}\mu_0^{(m)}\\ G_{22}^{(m)}\\ G_{23}^{(m)}\end{pmatrix},\quad \tilde{\tilde{H}}^{(m)}=\begin{pmatrix}0\\ 0\\ \Omega_{23}^{(m)}G_{23}^{(m)}\end{pmatrix},\quad \tilde{\tilde{\mu}}_1^{(m)}=\begin{pmatrix}\mu_1^{(m)}\\ 0\\ 0\end{pmatrix},\quad \tilde{\tilde{F}}^{(m)}=\begin{pmatrix}\mu^{(m)}\\ F_2^{(m)}\\ F_3^{(m)}\end{pmatrix}.$$

Meanwhile we eliminate $U_{2,m}$ from (20a) and (20c), which yields

$$\mu_0^{(m+1)}U_{2,m+1}+\mu_1^{(m+1)}U_{2,0}=\mu^{(m+1)},$$
$$\nu_0^{(m+1)}U_{2,m+1}+\nu_1^{(m+1)}U_{2,0}=\nu^{(m+1)}.$$

Noting that the two equations have the form (20d—e), and (20a—c) can always be obtained from (18a—c), we can repeat the above computation until $m=M-1$. At last we obtain

$$\begin{cases}\mu_0^{(M)}U_{2,M}+\mu_1^{(M)}U_{2,0}=\mu^{(M)},\\ \nu_0^{(M)}U_{2,M}+\nu_1^{(M)}U_{2,0}=\nu^{(M)}.\end{cases}\tag{22}$$

Obviously the expressions for $\mu_0^{(m+1)}, \cdots, \nu^{(m+1)}$ are of the following forms:

$$\begin{cases}\mu_0^{(m+1)}=G_{21}^{(m+1)}-\Omega_{21}^{(m+1)}G_{21}^{(m+1)}\tilde{\tilde{G}}^{(m)^{-1}}\tilde{\tilde{H}}^{(m)},\\ \mu_1^{(m+1)}=-\Omega_{21}^{(m+1)}G_{21}^{(m+1)}\tilde{\tilde{G}}^{(m)^{-1}}\tilde{\tilde{\mu}}_1^{(m)},\\ \mu^{(m+1)}=F_{21}^{(m+1)}-\Omega_{21}^{(m+1)}G_{21}^{(m+1)}\tilde{\tilde{G}}^{(m)^{-1}}\tilde{\tilde{F}}^{(m)},\\ \nu_0^{(m+1)}=-\nu_0^{(m)}\tilde{\tilde{G}}^{(m)^{-1}}\tilde{\tilde{H}}^{(m)},\\ \nu_1^{(m+1)}=\nu_1^{(m)}-\nu_0^{(m)}\tilde{\tilde{G}}^{(m)^{-1}}\tilde{\tilde{\mu}}_1^{(m)},\\ \nu^{(m+1)}=\nu^{(m)}-\nu_0^{(m)}\tilde{\tilde{G}}^{(m)^{-1}}\tilde{\tilde{F}}^{(m)}.\end{cases}\tag{23}$$

The process of elimination for (17) is the same as above. We only need to regard $\begin{pmatrix}G_{11}\\ G_{12}\end{pmatrix}$ as G_{21}, $\begin{pmatrix}\Omega_{11}, & 0\\ 0, & \Omega_{12}\end{pmatrix}$ as Ω_{21}, and $\begin{pmatrix}F_{11}\\ F_{12}\end{pmatrix}$ as F_{21}. By using the above expressions we can also obtain

$$U_{1,m}=\tilde{G}^{(m)^{-1}}\tilde{F}^{(m)}-\tilde{G}^{(m)^{-1}}\tilde{H}^{(m)}U_{1,m+1}-\tilde{G}^{(m)^{-1}}\tilde{\mu}_1^{(m)}U_{1,0}\tag{24}$$

and

$$\begin{cases}\mu_{01}^{(M)}U_{1,M}+\mu_{11}^{(M)}U_{1,0}=\mu_{21}^{(M)},\\ \mu_{02}^{(M)}U_{1,M}+\mu_{12}^{(M)}U_{1,0}=\mu_{22}^{(M)},\\ \nu_{01}^{(M)}U_{1,M}+\nu_{11}^{(M)}U_{1,0}=\nu_{21}^{(M)}.\end{cases}\tag{25}$$

2) Computation of the quantities on the boundaries.

Since the quantities in region 3 can be obtained before the quantities in the other two regions are evaluated, $U_{2,M}=U_{3,0}$ and $U_{2,M}$ can be easily determined. After $U_{2,M}$ is known, $U_{1,M}$, $U_{1,0}$, $U_{2,0}$ can be obtained by using (18b) with $m=M$, (22), (25), the relations on the contact discontinuity: $u_{1,M}=u_{2,0}$, $p_{1,M}=p_{2,0}$ and the relation on the incident shock $p_{1,0}=0.1\rho_{1,0}u_{1,0}^2$.

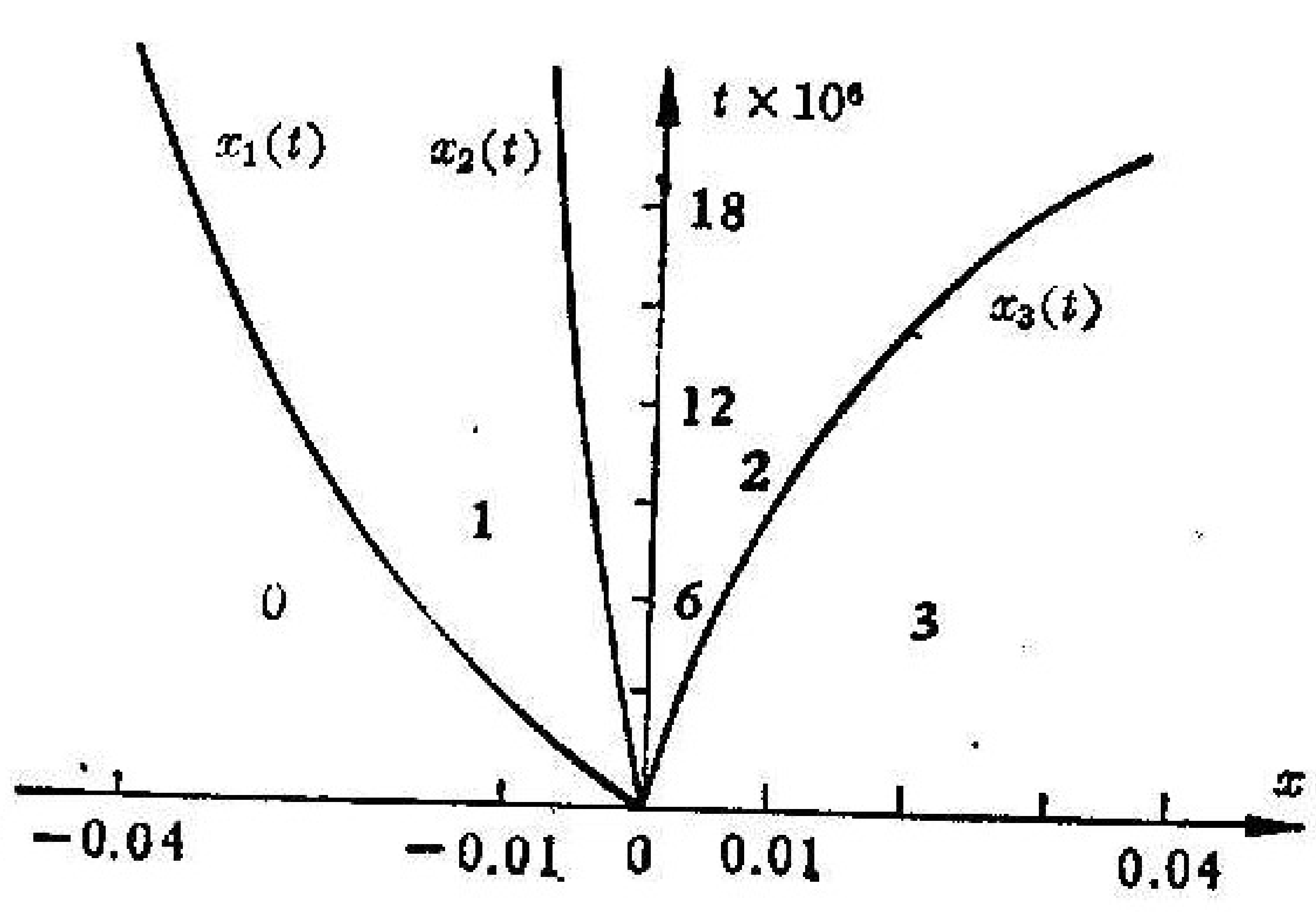

Fig. 4

3) Computation of the quantities of internal points in these subregions.

Using (21) and (24) we can easily obtain the quantities in region 1 and region 2.

Case II. Suppose that an incident $x_1(t)$, a contact discontinuity $x_2(t)$ and a reflected shock $x_3(t)$ are produced (see Fig. 4) when the strong explosion wave meets the boundary.

Here the case is similar to the previous case. We want to obtain the quantities in region 1 and region 2, the velocities and locations of three discontinuity surfaces. First we transform regions 1 and 2 into the strips $1\leqslant\xi\leqslant2$ and $2\leqslant\xi\leqslant3$ on the ξ-t plane by using the transformation in the above section. Then we compute the initial values in the two regions at $t=0$. Obviously, on the incident shock, the contact discontinuity and the reflected shock, there are the following relations respectively:

$$\begin{cases}\hat{\rho}_1=\dfrac{\gamma_l+1}{\gamma_l-1}\rho_0,\\ \hat{u}_1=\dfrac{2}{\gamma_l+1}V_1,\\ \hat{p}_1=\dfrac{\gamma_l+1}{2}\rho_0\hat{u}_1^2,\end{cases}$$

$$\begin{cases}\hat{u}_1=\hat{u}_2,\\ \hat{p}_1=\hat{p}_2,\end{cases}$$

and

$$\begin{cases}\hat{\rho}_2=\rho_{3,0}\dfrac{2\gamma_r+(\gamma_r+1)z}{2\gamma_r+(\gamma_r-1)z},\\ \hat{p}_2=(1+z)p_{3,0},\\ \hat{u}_2=u_{3,0}+\dfrac{z}{\gamma_r(1+(\gamma_r+1)z/(2\gamma_r))^{1/2}}\cdot c_{3,0}.\end{cases}$$

Here z is the strength of shock, and $u_{3,0}$, $\rho_{3,0}$, $p_{3,0}$, $c_{3,0}$ are the quantities in front of the reflected shock, which can be computed by using (8a—c). From the above relations, the following nonlinear equation for z can be obtained:

$$3\rho_0\left(u_{3,0}+\frac{z}{\gamma_r(1+(\gamma_r+1)z/(2\gamma_r))^{1/2}}\cdot c_{3,0}\right)^2=p_{3,0}(1+z). \tag{26}$$

Solving (26) we obtain z. Then $\hat{u}_2$, $\hat{\rho}_2$, $\hat{p}_2$, $\hat{u}_1$, $\hat{\rho}_1$, $\hat{p}_1$ can be obtained from the above relations. The velocities of three boundaries are $V_1=\dfrac{\gamma_l+1}{2}u_{1,0}$, $V_2=u_{2,0}$ and $V_3=u_{3,0}+(1+(\gamma_r+1)z/(2\gamma_r))^{1/2}c_{3,0}$.

In the same way as case I we can derive systems of difference equations. Using the double-sweep method to solve the system consisting of difference equations and the relations on the discontinuities, we can then obtain the quantities in regions 1 and 2.

In the above two cases the location of the boundaries can be determined using the following schemes with second order accuracy:

$$x_i^{k+\frac{1}{2}}=x_i^k+V_i^k\cdot\Delta t/2,$$
$$x_i^{k+1}=x_i^k+V_i^{k+\frac{1}{2}}\Delta t,$$

where V_i is the speed of the boundary x_i.

Since $x_{i+1}^0-x_i^0=0$ and λ contains $1/(x_{i+1}-x_i)$, λ is equal to infinity at $t=0$. In order to solve this problem we make the following revision: Because $x_i^{1/2}=x_i^0+V_i^0\cdot\Delta t/2$ can be obtained in advance, we may substitute $x_i^{1/2}$ for x_i^0 without causing any other problem. Thus the problem of the vanishing denominator can be averted.

In the computation we have estimated the fractional errors of mass, momentum and energy:

The error of mass $=\left(\int_{x_1}^{x_2}(\rho)_{t=t_2}dx-\int_{x_1}^{x_2}(\rho)_{t=t_1}dx-\int_{t_1}^{t_2}(\rho u)_{x=x_1}dt+\int_{t_1}^{t_2}(\rho u)_{x=x_2}dt\right)\Big/\int_{x_1}^{x_2}(\rho)_{t=t_2}dx$. The error of momentum $=\left(\int_{x_1}^{x_2}(\rho u)_{t=t_2}dx-\int_{x_1}^{x_2}(\rho u)_{t=t_1}dx-\int_{t_1}^{t_2}(\rho u^2+p)_{x=x_1}dt+\int_{t_1}^{t_2}(\rho u^2+p)_{x=x_2}dt\right)\Big/\int_{x_1}^{x_2}(\rho u)_{t=t_2}dx$. The error of energy $=\left(\int_{x_1}^{x_2}\rho\left(e+\frac{u^2}{2}\right)_{t=t_2}dx-\int_{x_1}^{x_2}\rho\left(e+\frac{u^2}{2}\right)_{t=t_1}dx-\int_{t_1}^{t_2}\left(\rho\left(e+\frac{u^2}{2}\right)u+pu\right)_{x=x_1}dt+\int_{t_1}^{t_2}\left(\rho\left(e+\frac{u^2}{2}\right)u+pu\right)_{x=x_2}dt\right)\Big/\int_{x_1}^{x_2}\rho\left(e+\frac{u^2}{2}\right)_{t=t_2}dx$.

We can easily obtain the values of above three errors using the numerical integration.

4. Numerical Results

We have computed the following three problems with different increments of the variable x and t by using the singularity-separating method.

A. Suppose that before the explosion, the state of gas at $x<0$ is $\gamma_l=1.2$, $\rho_l=0.6377$, $u_l=p_l=e_l=0$; at $x>0$, $\gamma_r=1.4$, $\rho_r=1.29$, $u_r=p_r=e_r=0$. As a result of

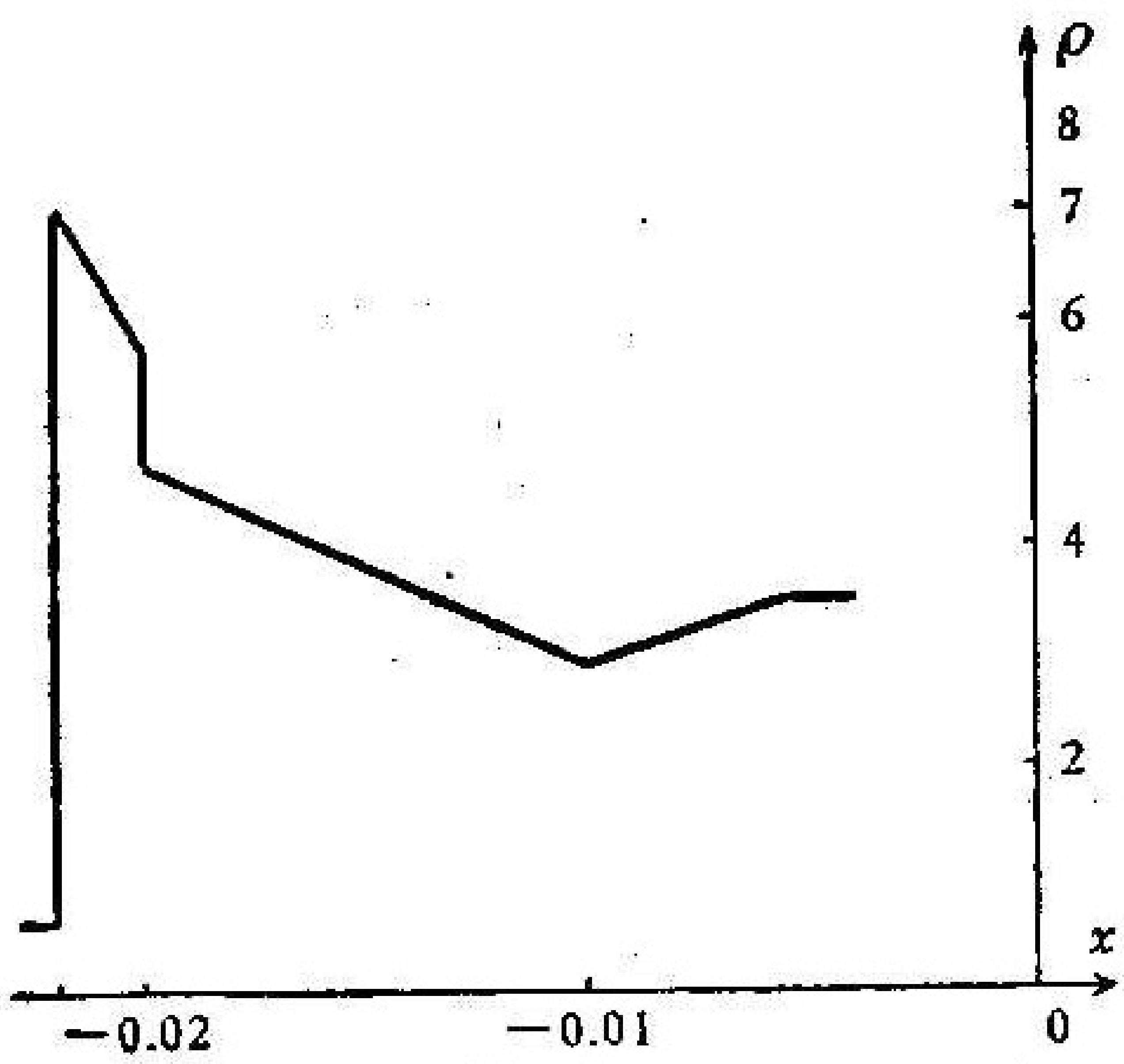

Fig. 5a

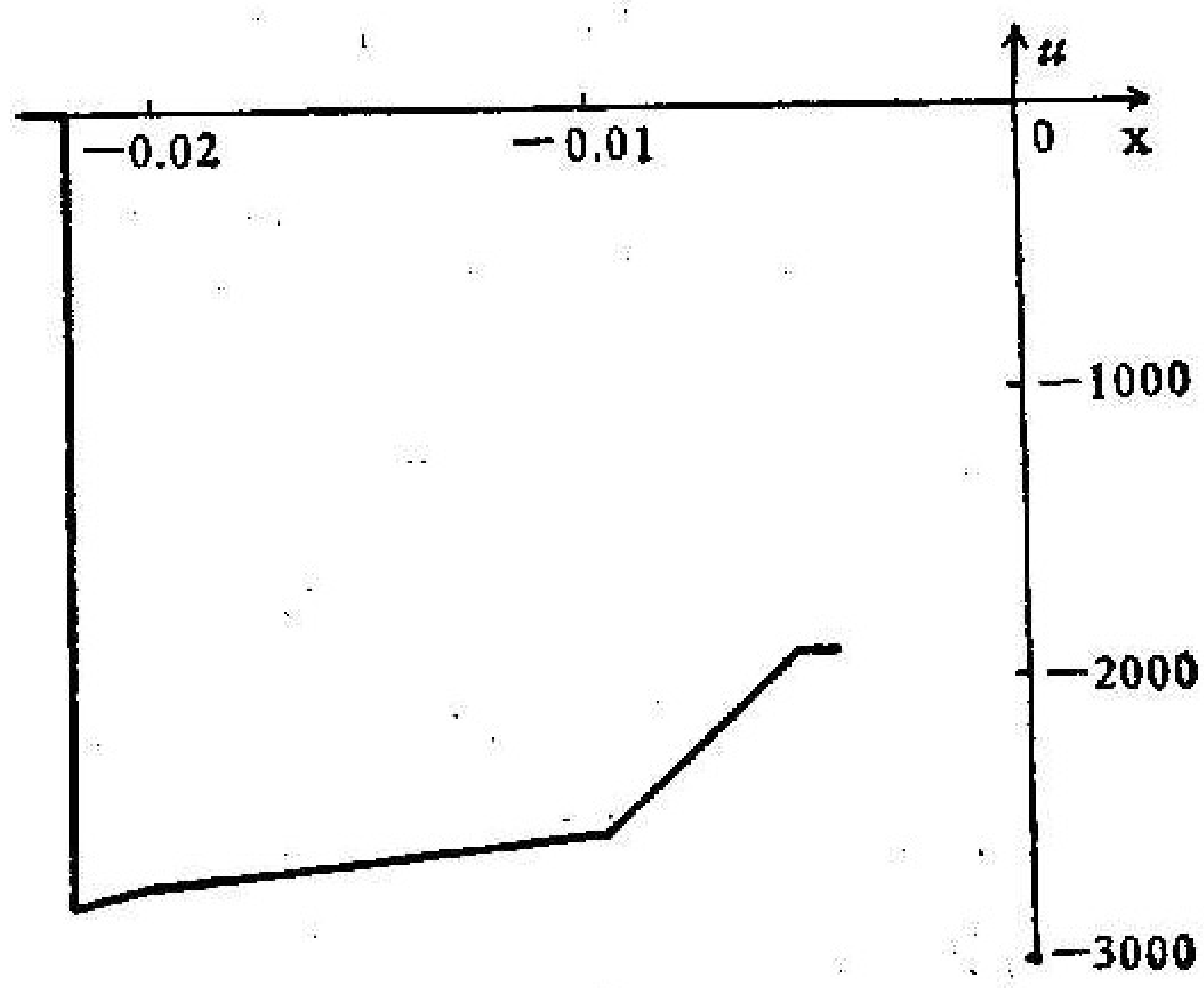

Fig. 5b

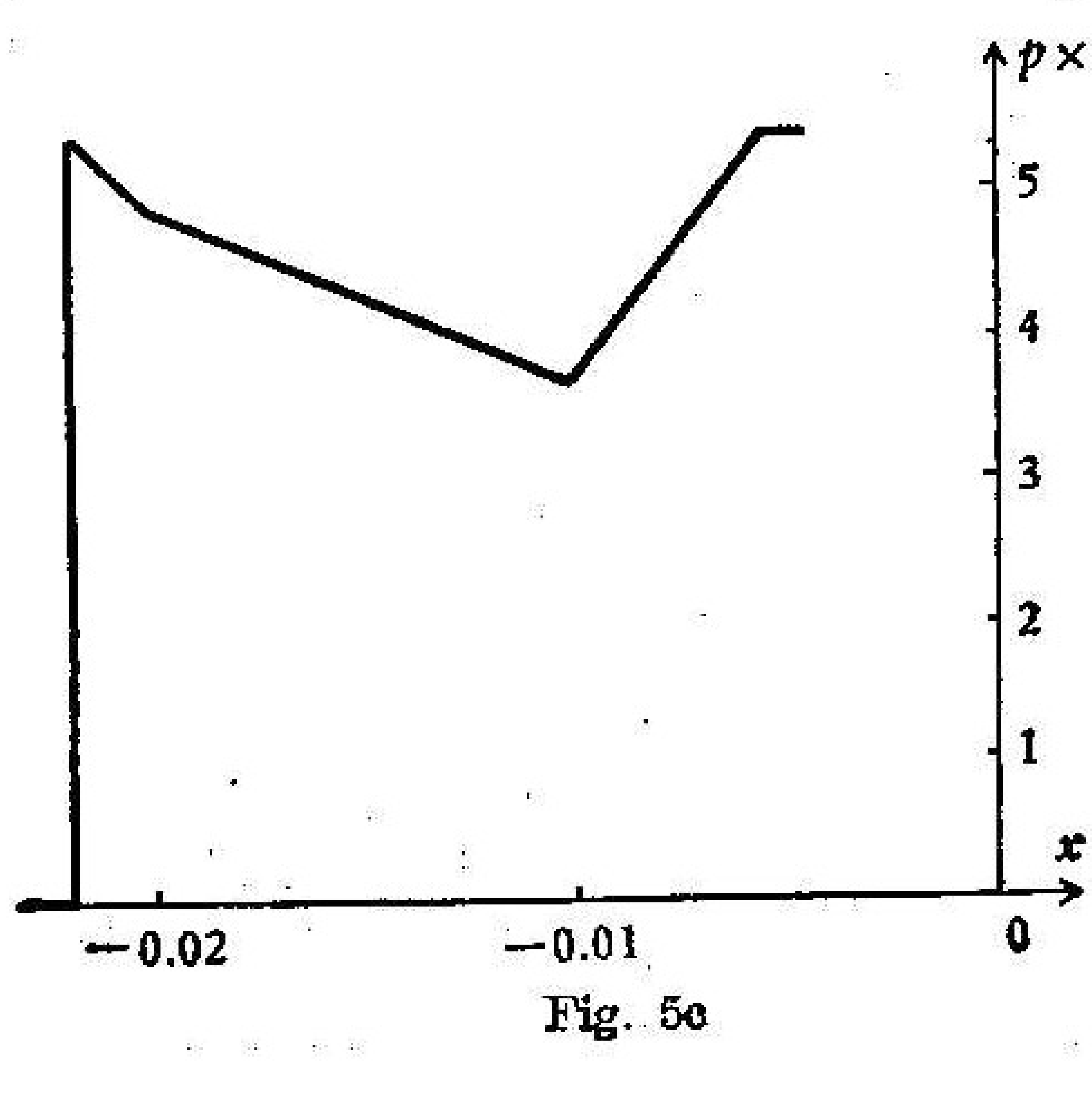

Fig. 5c

interaction between the strong explosion wave and the boundary, an incident shock, a contact discontinuity and a reflected rarefaction wave are produced. The case is the same as case I in section 3. Here, the initial values in each subregion are $\hat{\rho}_1=7.0147$, $\hat{\rho}_2=\rho_{3,0}=5.52$, $\rho_{3,M}=7.74$, $\hat{u}_1=\hat{u}_2=u_{3,0}=-3000$, $u_{3,M}=-2558$, $\hat{p}_1=\hat{p}_2=p_{3,0}=6.31323\times10^6$, $p_{3,M}=10129280$, $c_{3,M}=1353.6$. The initial speeds of four boundaries are $V_1=-3300$, $V_2=-3000$, $V_3=-1734$, $V_4=-1204$. Using the method given in case I we can obtain the quantities in three subregions at any time.

Table 1 shows the numerical solutions at $t=7\times10^{-6}$ with different increments of the variables x and t. From that table we can see that the solutions have three significant digits though a few mesh points and the large increment of the variable t are used. All the fractional errors of mass, momentum and energy are under 0.3%. This result shows that our computation is accurate. In Fig. 3 the locations of the discontinuities are described. Figs. 5a, b, c give for $t=7\times10^{-6}$ the distributions of density, velocity and pressure. From these figures we can see that the discontinuity fronts in the solutions obtained by using the singularity-separating method are sharp. The quantities in all subregions are smooth. There is no overshoot or undershoot. There is no smearing or oscillation.

Table 1. Contrast between the results in case A at $t=7\times10^{-6}$

M	Δt	x_1	x_2	x_3	x_4	$u_{1,0}$	$u_{1,M}$ $u_{2,0}$	$u_{2,M}$ $u_{3,0}$	$u_{3,M}$	$\rho_{1,0}$	$\rho_{1,M}$	$\rho_{2,0}$	$\rho_{2,M}$ $\rho_{3,0}$
40	2.5×10^{-8}	−0.02218	−0.01995	−0.01012	−0.00563	−2775	−2716	−2512	−1929	7.015	5.692	4.614	2.981
20	5×10^{-8}	−0.02218	−0.01994	−0.01012	−0.00563	−2774	−2715	−2512	−1928	7.015	5.691	4.611	2.979
10	10×10^{-8}	−0.02217	−0.01993	−0.01012	−0.00562	−2773	−2714	−2511	−1928	7.015	5.689	4.604	2.975

M	$\rho_{3,M}$	$p_{1,0}$	$p_{1,M}$ $p_{2,0}$	$p_{2,M}$ $p_{3,0}$	$p_{3,M}$	fractional error mass	fractional error momentum	fractional error energy
40	3.456	5400000	4913000	3717000	5424000	−0.00054	−0.00070	−0.00061
20	3.454	5398000	4911000	3715000	5423000	−0.0011	−0.0013	−0.0012
10	3.451	5394000	4907000	3712000	5420000	−0.0019	−0.0024	−0.0021

B. Suppose that before the explosion the state of gas is $\gamma_l=5$, $\rho_l=20.26$, $u_l=p_l=e_l=0$ at $x<0$ and $\gamma_r=1.4$, $\rho_r=1.29$, $u_r=e_r=p_r=0$ at $x>0$. As a result of interaction between the strong explosion wave and the boundary, an incident shock, a contact discontinuity and a reflected shock are produced. The case is the same as case II in section 3. Here, the initial values in each subregion are $\hat{\rho}_1=30.386$, $\hat{\rho}_2=20.64$, $\rho_{3,0}=7.74$, $\hat{p}_1=\hat{p}_2=45581760$, $p_{3,0}=10129280$, $\hat{u}_1=\hat{u}_2=V_2=-866.05$, $u_{3,0}=-2558$, $V_1=-2598.15$, $V_3=149.2$, $z=3.5$. Using the method given in case II we can obtain the quantities in two ssbregions at any time.

Table 2 shows the numerical solutions with different increments of the variables x and t at $t=6\times10^{-6}$. From this table we can see that the solutions also have three significant digits, but the fractional errors are smaller than those in case A. The locations of the discontinuities are described in Fig. 4. Figs. 6a, b, c give for $t=6\times10^{-6}$ the distributions of density, velocity and pressure.

Table 2. Contrast between the results in case B at $t=6\times10^{-6}$

M	Δt	x_1	x_2	x_3	$u_{1,0}$	$u_{1,M}$ $u_{2,0}$	$u_{2,M}$	$u_{3,0}$	$\rho_{1,0}$	$\rho_{1,M}$	$\rho_{2,0}$
40	1.25×10^{-8}	−0.01439	−0.004072	0.004629	−744.7	−534.0	86.13	−1758.2	30.386	26.146	12.066
20	2.5×10^{-8}	−0.01439	−0.004072	0.004629	−744.7	−534.0	86.10	−1758.2	30.386	26.146	12.066
10	5×10^{-8}	−0.01439	−0.004072	0.004628	−744.7	−534.0	85.97	−1758.3	30.386	26.146	12.066

M	$\rho_{2,M}$	$\rho_{3,0}$	$p_{1,0}$	$p_{1,M}$ $p_{2,0}$	$p_{2,M}$	$p_{3,0}$	fractional error		
							mass	momentum	energy
40	5.9295	2.4061	33705000	22499000	18525000	4750800	−0.0000015	0.000014	−0.0000036
20	5.9295	2.4061	33704000	22498000	18524000	4750800	−0.0000055	0.000055	−0.000012
10	5.9293	2.4061	33701000	22495000	18523000	4750900	−0.000019	0.00022	−0.000038

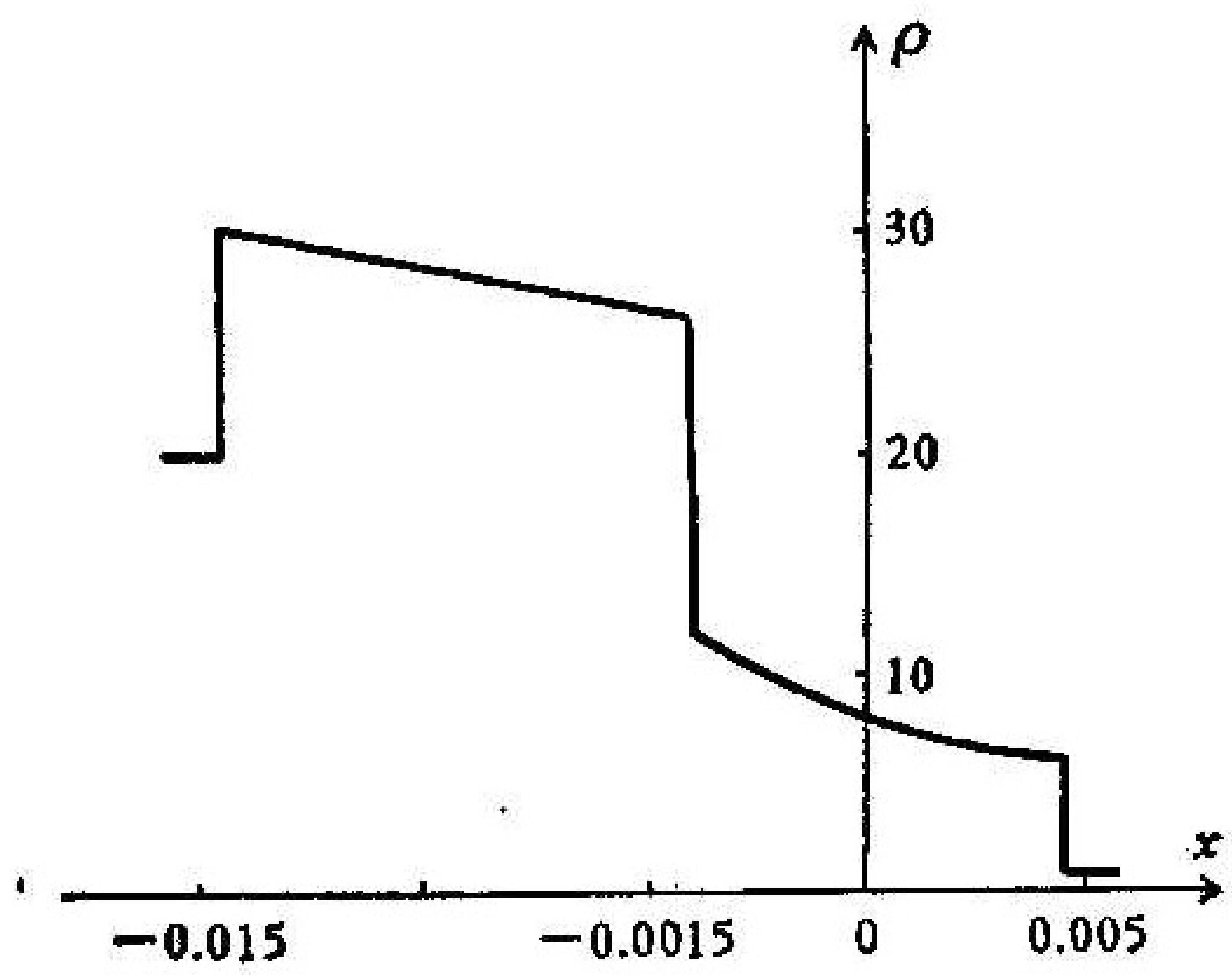

Fig. 6a

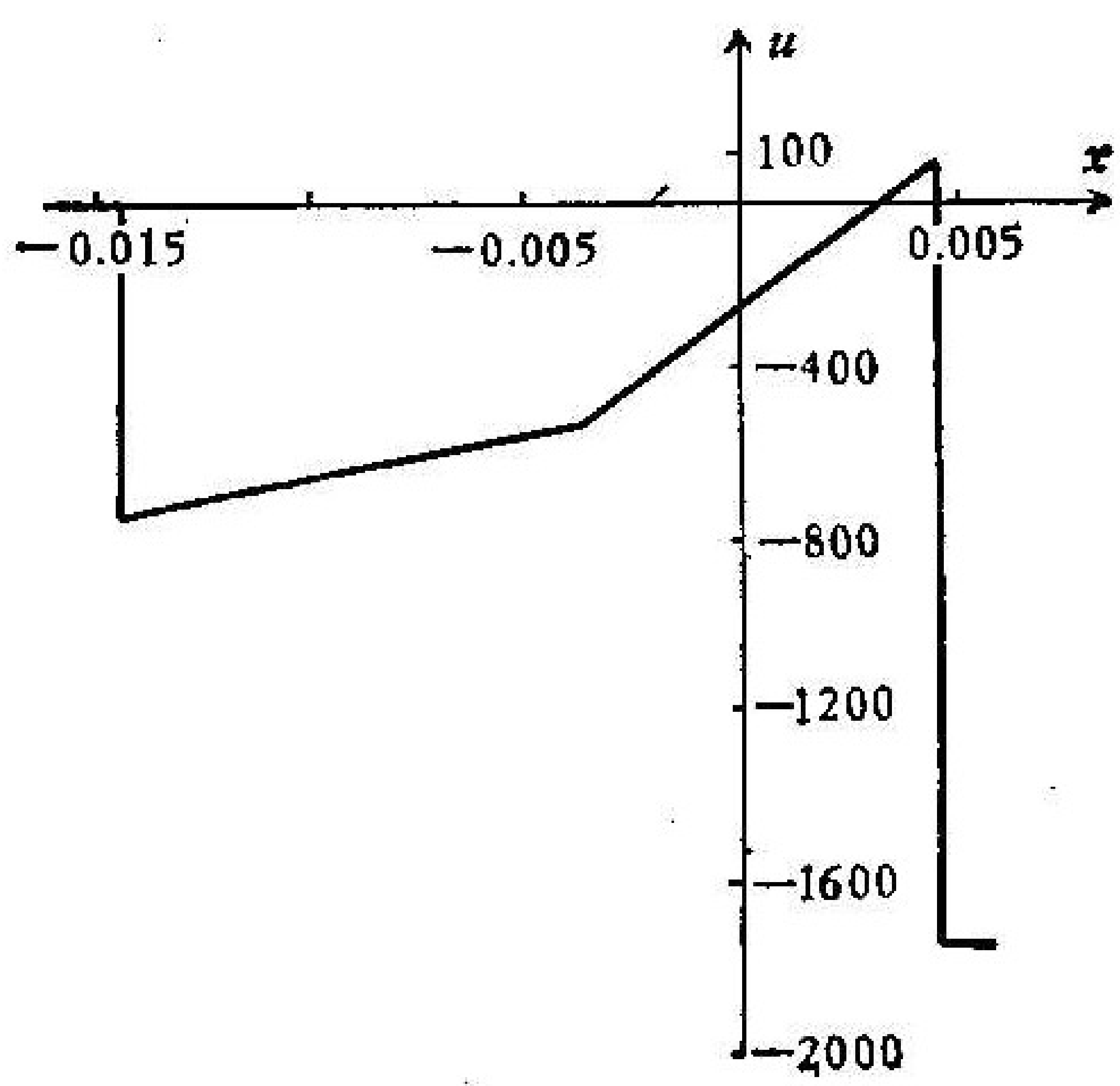

Fig. 6b

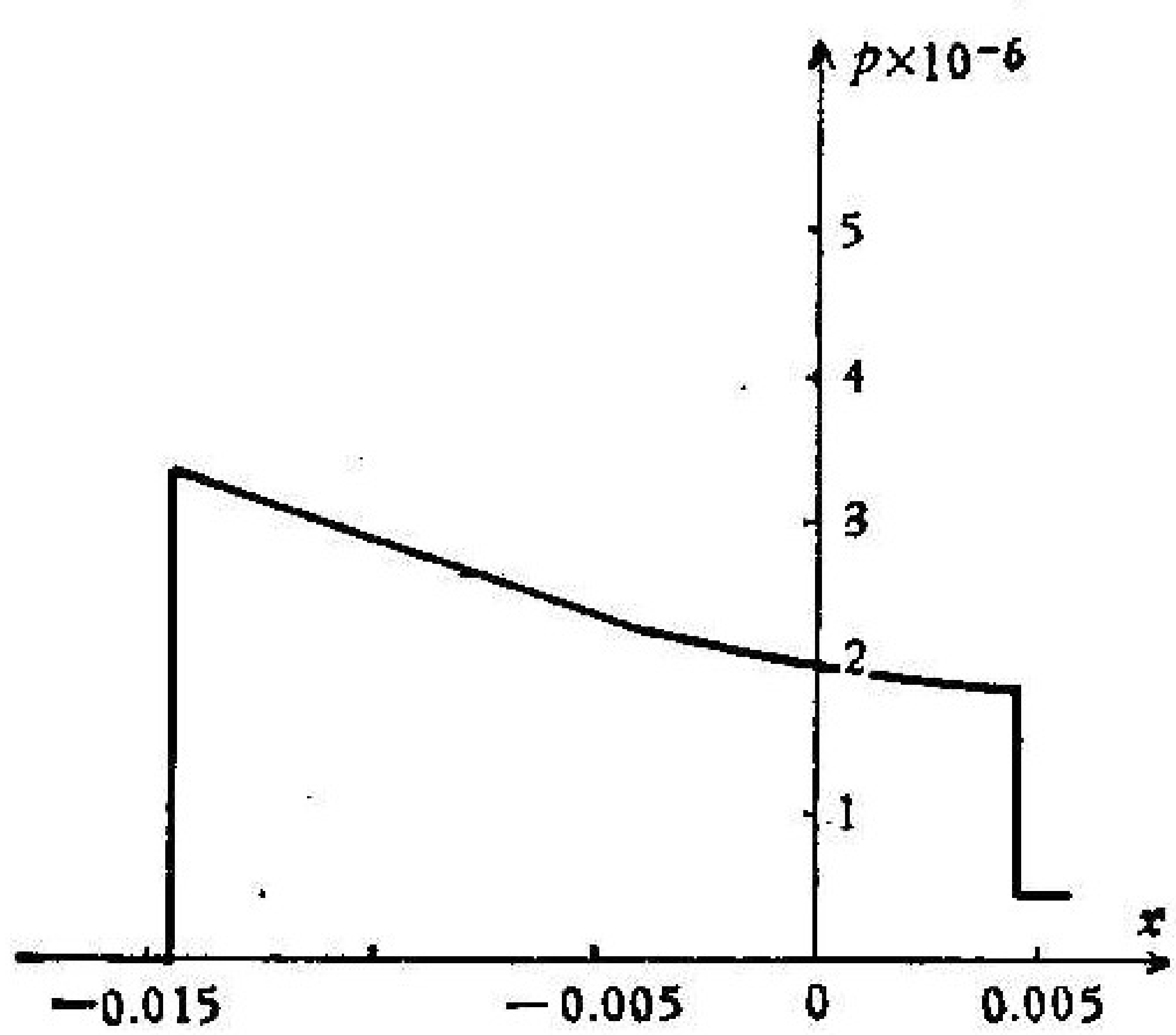

Fig. 6c

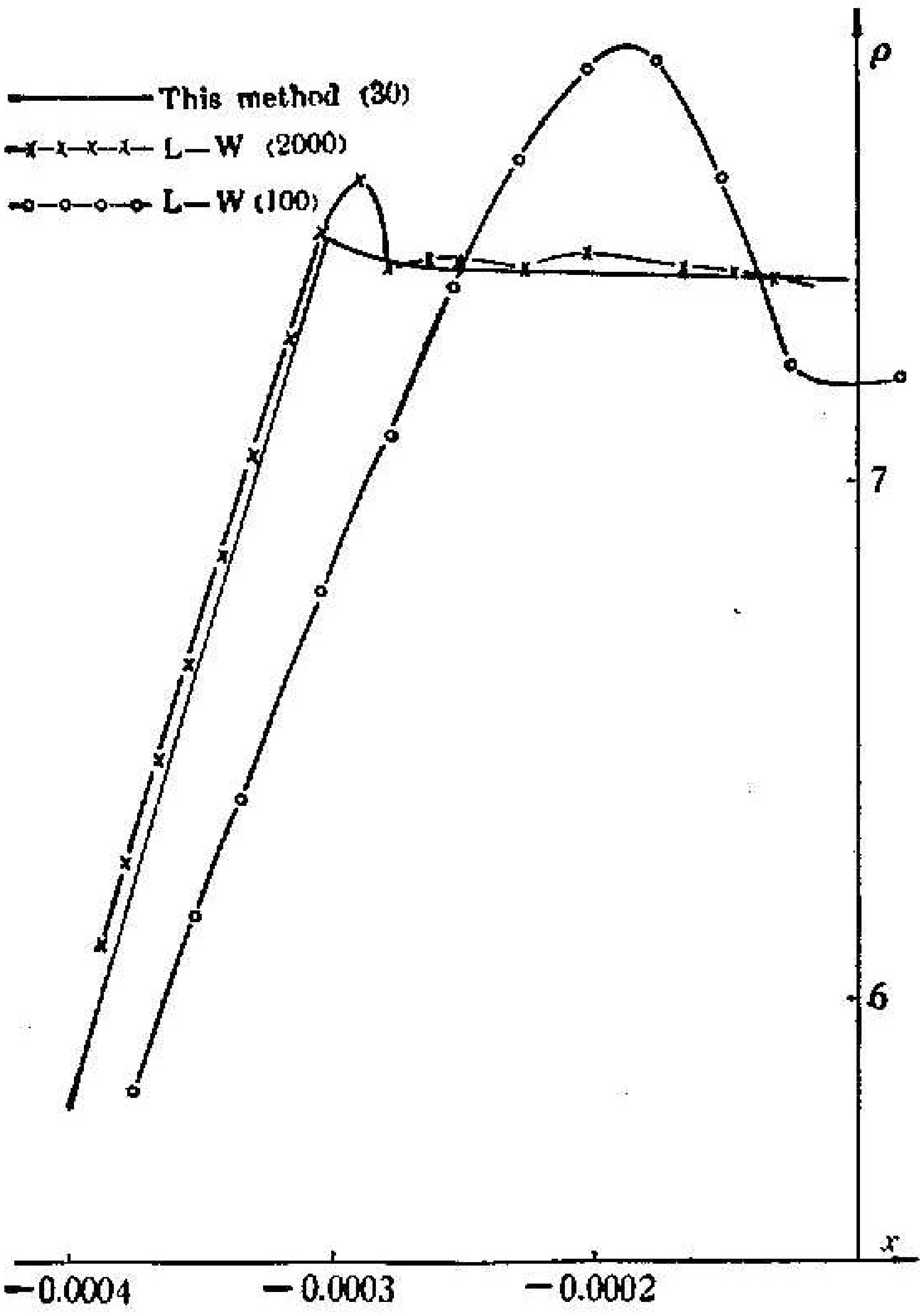

Fig. 7a

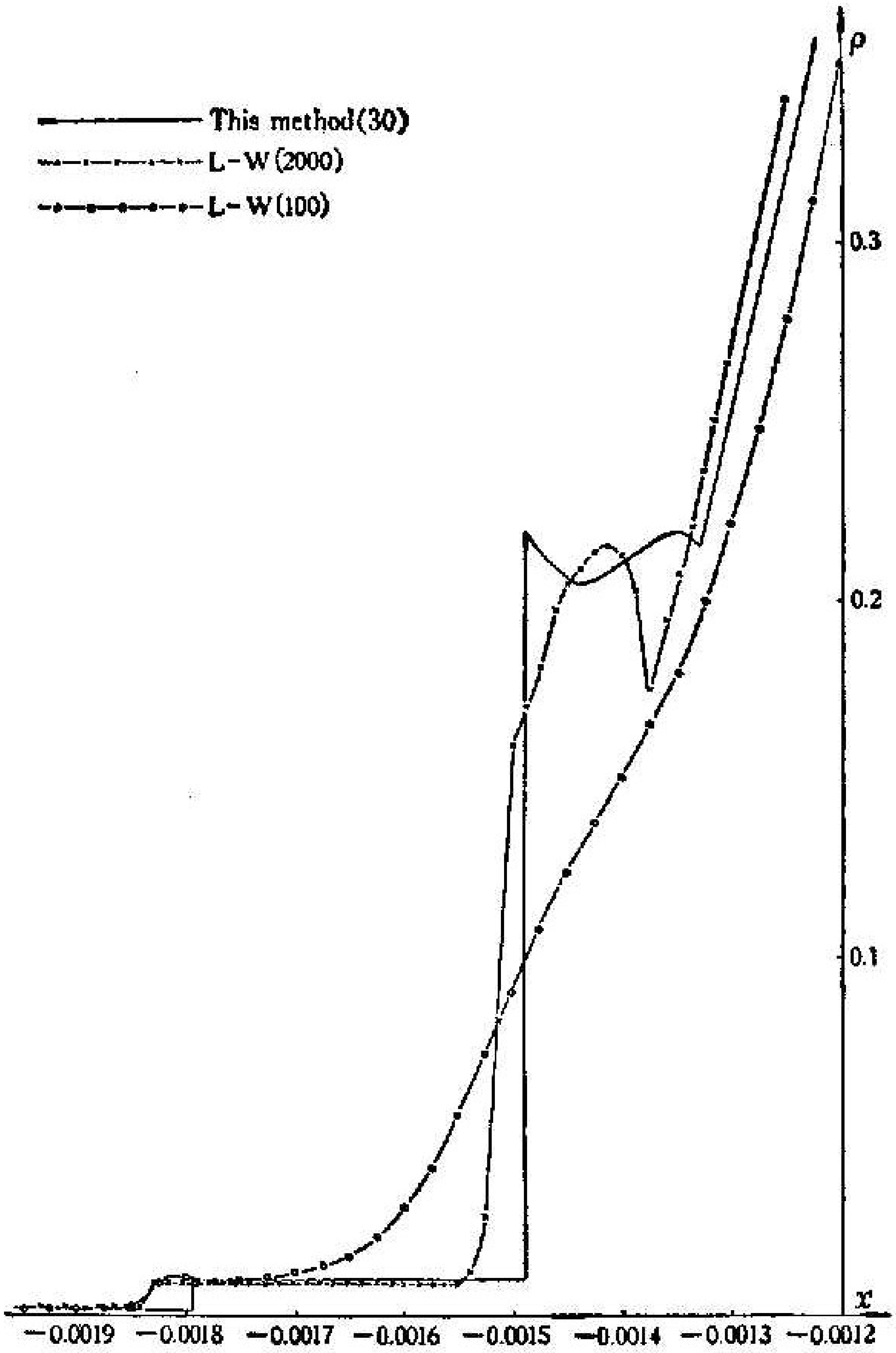

Fig. 7b

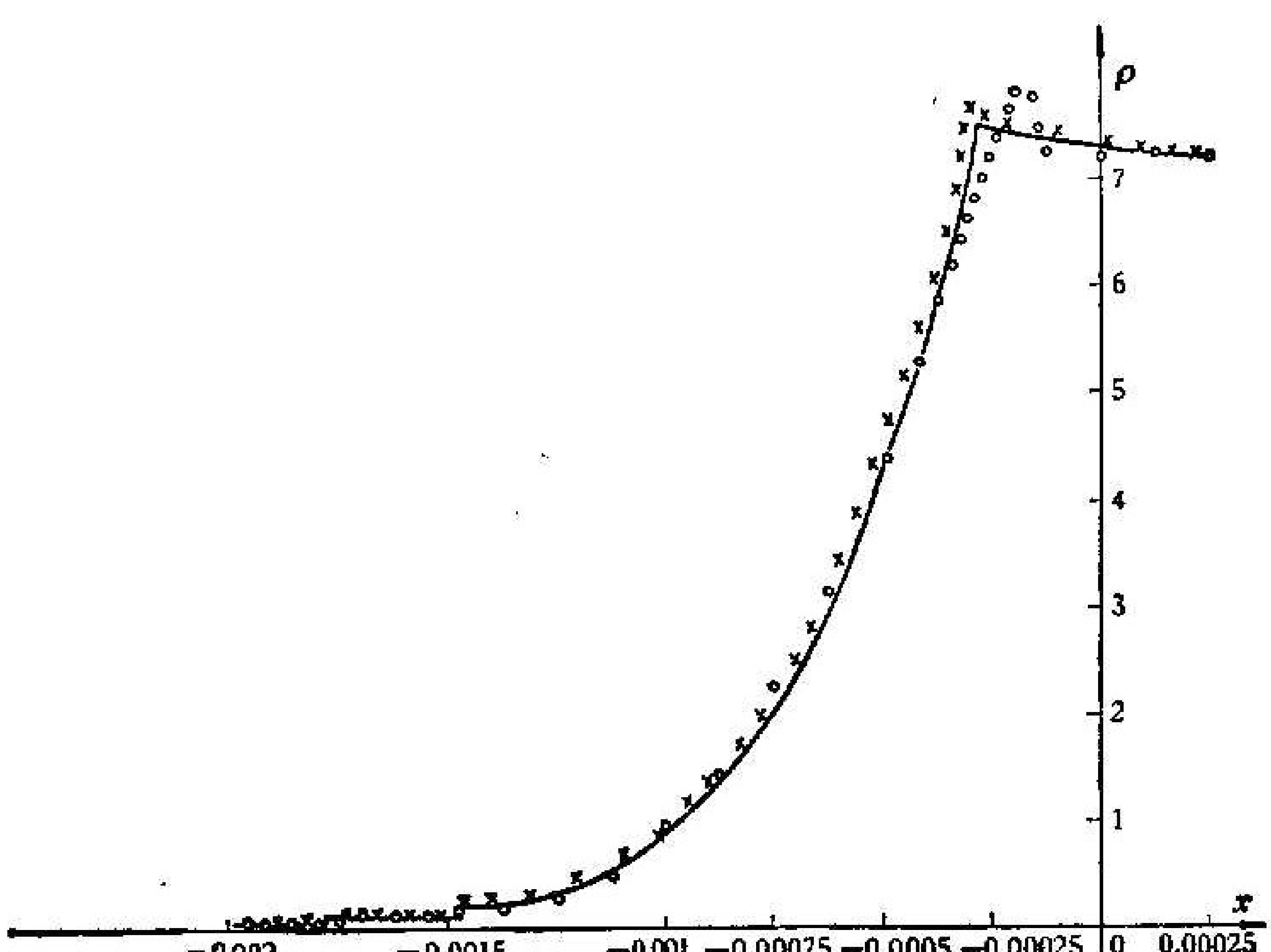

Fig. 7c

C. In order to compare our scheme with the *L–W* scheme we have also solved the following single medium flow problem with interaction between a shock and a contact discontinuity. Suppose that before the explosion, the state of the gas is $\gamma_l=1.4$, $\rho_l=0.0016$, $u_l=p_l=e_l=0$, at $x<0$ and $\gamma_r=1.4$, $\rho_r=1.24$, $u_r=p_r=e_r=0$, at $x>0$. As a result of interaction between the shock and the contact discontinuity, an incident shock, a contact discontinuity and a reflected rarefaction wave are produced. The case is the same as case I in section 3. Here, the initial values in each subregion are $\hat{u}_1=\hat{u}_2=u_{3,0}=-6000$, $\hat{p}_1=\hat{p}_2=p_{3,0}=70110$, $\hat{\rho}_1=0.0097$, $\hat{\rho}_2=\rho_{3,0}=0.222$, $u_{3,M}=-2558$, $\rho_{3,M}=7.74$, $p_{3,M}=10129280$. Using the method in case I we can obtain the quantities in three subregions at any time.

The distribution of density for $t=2.5\times10^{-7}$ is described in Fig. 7a. Figs. 7b, 7c show the distributions of density obtained by this method and the *L–W* scheme in the subregion containing the shock and the contact discontinuity and in the subregion containing the end part of the rarefaction wave. Here we take the following increments for the *L–W* scheme: 100 mesh points in x-axis, i. e., $\Delta x\approx0.000025$, $\Delta t\approx0.217\times10^{-8}$ or 2000 mesh points in x-axis, i. e., $\Delta x\approx0.00000125$, $\Delta t\approx0.115\times10^{-9}$. In our scheme we take 30 mesh points in x-axis, i. e., $\Delta x\approx0.000017\sim0.0001$ (x in each subregion is not the same), $\Delta t=0.5\times10^{-7}$. These figures show that for the *L–W* scheme, if 100 mesh points are taken, the contact discontinuity is seriously smeared, and even if 2000 mesh points are taken, the contact discontinuity is still obviously smeared; and on the shock and the rarefaction wave there are quite large overshoots. However, taking tens of mesh points, one can obtain very accurate results if our method is used.

Here, the *L–W* scheme is

$$U_{m+\frac{1}{2}}^{k+\frac{1}{2}}=\frac{1}{2}(U_m^k+U_{m+1}^k)-\frac{\Delta t}{2\Delta x}(F_{m+1}^k-F_m^k),$$

$$U_m^{k+1}=U_m^k-\frac{\Delta t}{\Delta x}(F_{m+\frac{1}{2}}^{k+\frac{1}{2}}-F_{m-\frac{1}{2}}^{k+\frac{1}{2}}),$$

$$U=\begin{pmatrix}\rho\\ \rho u\\ \dfrac{p}{\gamma-1}+\dfrac{1}{2}\rho u^2\end{pmatrix},\quad F=\begin{pmatrix}\rho u\\ \rho u^2+p\\ u\left(\dfrac{\gamma}{\gamma-1}p+\dfrac{1}{2}\rho u^2\right)\end{pmatrix}.$$

The above numerical results show that the singularity-separating method is successful in computing discontinuous solutions not only in the case of single medium flow but also in the case of multimedium flow.

References

[1] Zhu You-lan, Zhong Xi-chang, Chen Bing-mu, Zhang Zuo-min, Difference methods for initial-boundary value problems and flow around bodies, Science Press, Beijing, China, 1980.

[2] Huang Dun, Normal reflection of a plane strong explosion wave, "Explosion and shock waves", Vol. 1, 18, 1981. (in Chinese)

[3] L. I. Sedov, Similarity and dimensional methods in mechanics, 1957. (in Russian)